Journal of Ceramic Processing Research. Vol. 21, Special. 1, pp. s47~s52 (2020)
(Received 16 December 2019, Received in revised form 21 April 2020, Accepted 4 May 2020)
https://doi.org/10.36410/jcpr.2020.21.S1.s47

J O U R N A L O F
Ceramic Processing Research

Effect of gas condition on graphene synthesized by rapid thermal chemical vapor deposition

Yang Soo Lee[a,†], Dong In Jeong[a,†], Yeojoon Yoon[b,†], Byeongmin Baek[c], Hyung Wook Choi[d], Seok Bin Kwon[a], Do Hun Kim[c], Young Joon Hong[e], Won Kyu Park[f], Young Hyun Song[g], Bong Kyun Kang[c], Dae Ho Yoon[a,*] and Woo Seok Yang[c,*]

[a]*School of Advanced Materials Science and Engineering, Sungkyunkwan University, Suwon 440-746, Republic of Korea*
[b]*Department of Environmental Engineering, Yonsei University, Wonju-si, Gangwon-do, Republic of Korea*
[c]*Nano Materials and Components Research Center, Korea Electronics Technology Institute, Seongnam-si, Gyeonggi-do 13509, Republic of Korea*
[d]*SKKU Advanced Institute of Nanotechnology (SAINT), Sungkyunkwan University, Suwon 16419, Korea*
[e]*Department of Nanotechnology and Advanced Material Engineering, Sejong University, Seoul 05006, Republic of Korea*
[f]*Nano Material Division, Cheorwon Plasma Research Institute, Cheorwon, Gangwon, 24047, Republic of Korea*
[g]*Lighting Design & Component Research Center, Korea Photonics Technology Institute, Gwangju 61007, Republic of Korea*

Graphene was synthesized using rapid thermal chemical vapor deposition (RT-CVD) equipment designed to produce large-area graphene at high speed. The effects of methane (CH_4), argon (Ar), and hydrogen (H_2) gases were investigated between 800 ºC and 1,000 ºC during heating and cooling in the graphene synthesis process. The findings reveal that multilayer domains increased due to hydrogen pretreatment with increase in temperature. Furthermore, when pretreated with the same gas, it was confirmed that the post-argon-treated sample cooled from 1,000 ºC to 800 ºC had a higher I_D/I_G value than that of the other samples. This result was consistent with the sheet resistance properties of graphene. The sample prepared in methane atmosphere maintained during both the pre-treatment and post-treatment demonstrated the lowest sheet resistance of 787.49 Ω/sq. Maintaining the methane gas atmosphere in the high-temperature region during graphene synthesis by RT-CVD reduced the defects and improved the electrical property.

Keywords: Graphene, Rapid thermal chemical vapor deposition, Gas condition.

Introduction

The progress in information and communication technology has led to the rapid development of electronic materials industry [1]. With the growing popularity of smart devices, research on high performance and light-weight products has rapidly increased in the last several years. Carbon materials (carbon nanotube, graphene, g–C_3N_4) have attracted tremendous attention as high value-added materials due to their lightweight, higher strength, good chemical, and thermal stability properties compared to other materials [2, 3]. In addition, its excellent electrical properties and chemical stability makes a potential candidate for energy storage, batteries and electrode materials [4-6].

Especially, graphene, sp^2-hybridized carbon atoms, has superior electronic, optical, thermal, and mechanical properties [7, 8].

To effectively apply the various excellent properties of graphene to electronic materials, it is necessary to study the conditions of graphene synthesis process [9]. Chemical vapor deposition (CVD) is a suitable method for producing large-scale single-layer graphene [10, 11]. Graphene synthesized by CVD is a polycrystalline material, in which several micrometer-scale domains consisting of carbon, grow in two dimensions. Also, CVD method has been conducted to achieve uniform growth of single and large area carbon films on the transition metal surface at relatively low process costs [11-13]. During CVD synthesis of graphene, the synthetic conditions such as gas used, temperature, and pressure, affect the characteristics of the graphene synthesized. Therefore, investigating the synthesis mechanism of large-area and high-quality graphene is necessary to effectively apply the excellent properties of graphene to transparent electrodes and various electronic devices [5, 14].

However, thin film synthesis in conventional thermal CVD (T-CVD) equipment is time consuming, hindering the commercialization of monolayer graphene. Thus, the rapid thermal chemical vapor deposition (RT-CVD, RHP400V, NPS Corporation) equipment is suitable for

†Contributed equally to this work.
*Corresponding author:
Tel./Fax: +82-31-290-7388 (D. Yoon), +82-31-789-7057 (W. Yang)
E-mail: dhyoon@skku.edu (D. Yoon); wsyang@keti.re.kr (W.Yang)

graphene synthesis on the surfaces of large-area metal catalysts [15]. Furthermore, the RT-CVD could synthesize the graphene film about 7 times faster than the conventional T-CVD equipment [15]. Since the RT-CVD equipment is not widely available, there have been limited studies on the suitable process conditions for high-speed graphene synthesis. To investigate the properties of synthesized graphene using the RT-CVD, have been analyzed such as the crystal structure, defects, optical properties, and electrical properties [16, 17].

Process conditions such as temperature, gas, and pressure affect the properties of chemical-vapor-deposition materials [18-20]. The optimum ratio of hydrocarbon gas to hydrogen gas promotes the synthesis of low-defect monolayer graphene on copper foils, which was determined by the interaction between graphene growth and etching [21]. Especially, hydrogen plays an important role in the growth process of graphene by CVD as an activator for size-limited graphene domain growth and carbon adsorption on the surface of copper foils [21, 22]. Furthermore, the synthesis of graphene using a high purity methane precursor was reported at 800 ºC, which is lower than the typical temperature for graphene synthesis [23].

In this study, the graphene was synthesized in various gas conditions and growth temperatures (800 ºC ~ 1,000 ºC) by RT-CVD. In addition, to understand the effect of methane (hydrocarbon precursor), hydrogen, and argon (inert gas) on graphene synthesized by RT-CVD process, the synthetic processes were divided into 5 steps. The characteristics of graphene on various growth conditions was investigated.

Experimental

Graphene synthesis was performed using a RT-CVD system (RHP400V, NPS Corporation). Fig. 1 show the schematic of RT-CVD furnace. Since the RT-CVD system is equipped with several linear heating elements, it can heat up to over 7 times faster than a typical CVD furnace. Graphene was grown on the surface of a rolled copper foil (Nippon Mining & Metals Corporation, at least 99.9%) having a thickness of 0.035 mm, width of 350 mm, and length of 480 mm.

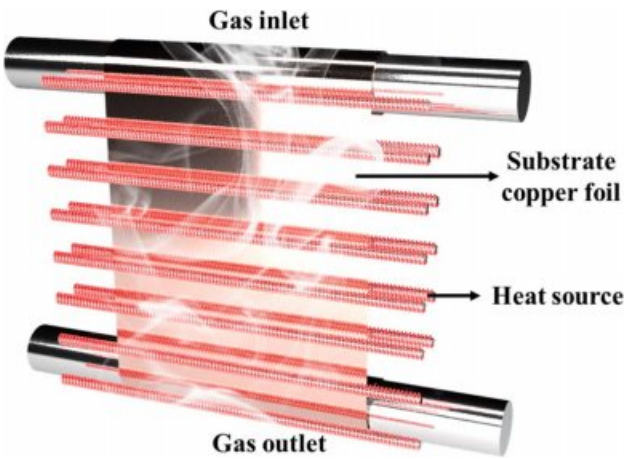

Fig. 1. Schematic of RT-CVD furnace capable of synthesizing large-area graphene faster.

Within the CVD equipment, the carbon precursor was adsorbed on both sides of the copper foil. To obtain monolayer graphene, the graphene grown on one side of the copper foil was etched with oxygen plasma for 10 s at a pressure of 110 mTorr and with 50 W RF power using reactive ion etching equipment (SciEnTech Co., Ltd.). To prevent the tearing of graphene after the etching of the copper foil, polymethyl methacrylate (PMMA) was spin coated on the graphene with a spin coater at 4,000 rpm for 30 s. The PMMA coated graphene/Cu sample was thermally cured at 180 ºC for 1 min using a hot plate. A silicon wafer coated with a 300-nm-thick oxide layer was sonicated in Standard Cleaning-1 (SC-1) solution ($NH_4OH:H_2O_2:H_2O$ = 1:1:5). The PMMA-coated thermally cured graphene/Cu samples were then etched with ammonium persulfate (APS) solution for 8 h. The APS solution was prepared by dissolving 32 g of APS powder in 2 L of deionized water. The PMMA-coated graphene film was washed with DI water and transferred to the SiO_2/Si wafer. Finally, the PMMA was removed with acetone for about 3 h.

Characterization

The morphology of the synthesized graphene was measured using a field emission scanning electron microscope (FE-SEM, JSM-700F, JEOL). High purity (99.999%) commercial argon, hydrogen (MS DONGMIN SPECIALTY GAS Ltd.), and methane (KOREA NOBLE GAS CO.) gas were used. The absorbance spectrum of graphene was measured using a UV-visible spectrophotometer (Cary 60 UV-Vis, Agilent Technologies). The electronic structure of graphene was evaluated using a Raman spectroscopy (Confotec MR520, SOL instruments) with a 532 nm laser source, and the electrical properties of graphene were measured using a four-point probe instrument (Loresta-GP/MCP-T610, Mitsubishi Chemical Analytech Co.).

Results and Discussion

The synthesis process was separated into 5 steps to analyze the impact of the different gas species on graphene properties at 800 ºC and 1,000 ºC. In all the graphene synthesis processes, the RT-CVD chamber was evacuated and maintained to 550 mTorr using a rotary vacuum pump.

At the beginning of the process (Table. 1), It was heat up to 800 ºC from room temperature, at a heating rate of 140 ºC/min in an atmosphere of 30 sccm Ar flowing (Step1). Next, the copper foil was thermally

Table 1. Process conditions of graphene synthesized using RT-CVD.

Case	Step 1	Step 2	Step 3	Step 4
Case I	Ar 30 sccm	CH_4 30 sccm	CH_4 30 sccm	CH_4 30 sccm
Case II	Ar 30 sccm	CH_4 30 sccm	CH_4 30 sccm	Ar 30 sccm
Case III	Ar 30 sccm	CH_4 30 sccm	CH_4 30 sccm	H_2 30 sccm
Case IV	Ar 30 sccm	Ar 30 sccm	CH_4 30 sccm	CH_4 30 sccm
Case V	Ar 30 sccm	Ar 30 sccm	CH_4 30 sccm	Ar 30 sccm
Case VI	Ar 30 sccm	Ar 30 sccm	CH_4 30 sccm	H_2 30 sccm
Case VII	Ar 30 sccm	H_2 30 sccm	CH_4 30 sccm	CH_4 30 sccm
Case VIII	Ar 30 sccm	H_2 30 sccm	CH_4 30 sccm	Ar 30 sccm
Case IX	Ar 30 sccm	H_2 30 sccm	CH_4 30 sccm	H_2 30 sccm

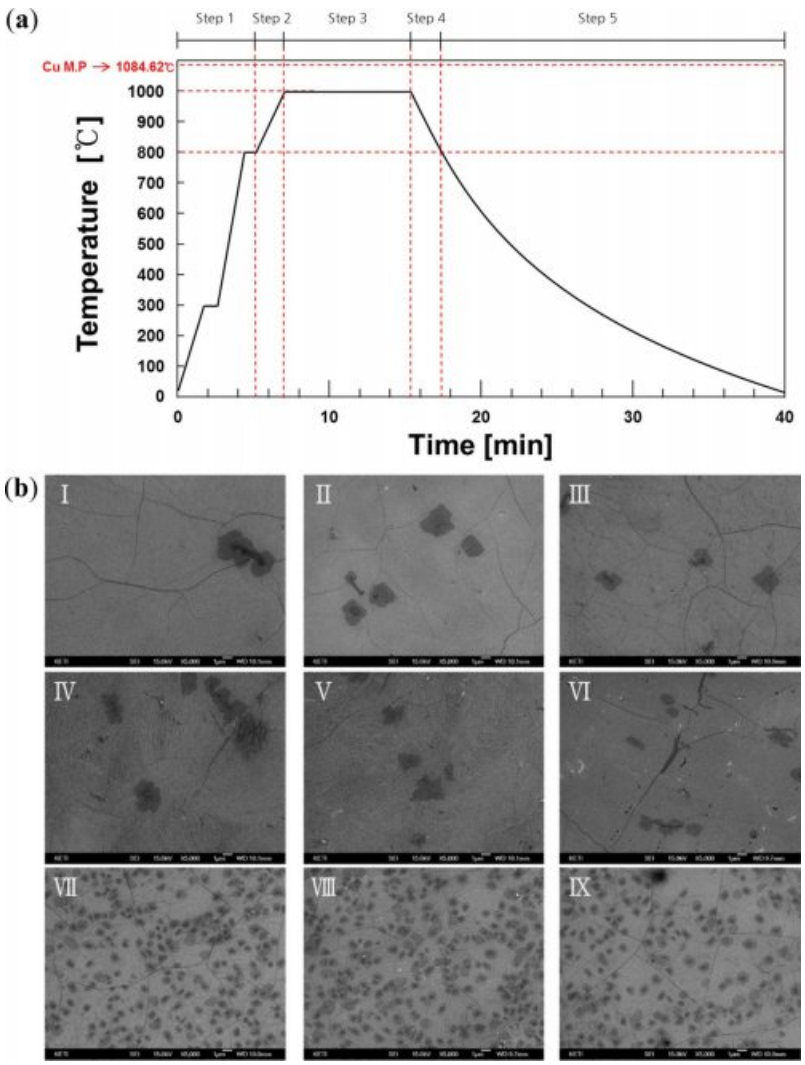

Fig. 2. (a) Process steps of graphene synthesis using RT-CVD. And (b) FE-SEM images of graphene synthesized in nine different gas conditions; Sample I: CH_4-CH_4, Sample II: CH_4-Ar, Sample III: CH_4-H_2, Sample IV: Ar-CH_4, Sample V: Ar-Ar, Sample VI: Ar-H_2, Sample VII: H_2-CH_4, Sample VIII: H_2-Ar, Sample IX: H_2-H_2.

treated from 800 ºC to 1,000 ºC under CH_4, Ar, and H_2 gases at an atmosphere of 30 sccm gas flowing (Step2). Graphene was synthesized at 1,000 ºC for 500 seconds in an atmosphere of 30 sccm CH_4 flowing (Step3). After the completion of graphene growth, an atmosphere of 30 sccm of CH_4, Ar, and H_2 gases were flowed while lowering the temperature of the copper foil from 1,000 ºC to 800 ºC (Step4). Finally, the CVD chamber was cooled from 800 ºC to room temperature with continuous N_2 flow at the rate of 1,0000 sccm. Fig. 2(a) shows the temperature conditions of the RT-CVD synthesis process. The gas conditions were as follows:

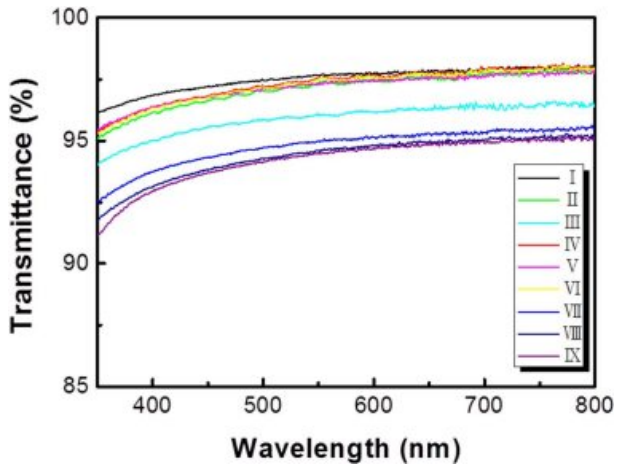

Fig. 3. Optical transmittance of graphene synthesized in nine different gas conditions.

Sample I: CH_4 (step2)-CH_4 (step4) flow, Sample II: CH_4-Ar, Sample III: CH_4-H_2, Sample IV: Ar-CH_4, Sample V: Ar-Ar, Sample VI: Ar-H_2, Sample VII: H_2-CH_4, Sample VIII: H_2-Ar, and Sample IX: H_2-H_2, respectively. The FE-SEM surface images of graphene transferred onto the silicon wafer were as shown in Fig. 2(b). The FE-SEM images of samples VII, VIII, and IX show the formation of numerous multilayer graphene domains when hydrogen gas was introduced in Step2. Graphene was synthesized by methane and the remaining hydrogen promoted the formation of multilayer graphene on the surface of the transition metal catalyst in Step3 [21].

The optical properties of the synthesized graphene are shown in Fig. 3. For samples VII, VIII, and IX, in which multilayer domains were formed due to hydrogen pretreatment, the measured transmittances were 94.97, 94.60, and 94.48%, respectively, and indicated an average absorption rate of 5.32% (at 550 nm). In contrast, sample I exhibited the best transparency (97.64%). Graphene was found to absorb approximately 2.3% of incident white light [24, 25]. It was concluded that the graphene domain islands with about 2~3 layers decreased the light transmittance. Due to the effects of residual hydrogen and methane on fast process rates, the domain density can be increased. Lower nucleation barriers can increase graphene nucleation density on the copper oxide compared with that ramped up and annealed on gas conditions without hydrogen [21].

The statistical analyses of Raman spectral data of graphene grown in nine different gas conditions were as presented in Fig. 4. Raman spectroscopy can provide information about the lattice structure of the target material using single frequency light such as a laser. The main features in the Raman spectra of carbon were the D peaks (1,350 cm^{-1}), G peaks (1,580 cm^{-1}) and 2D peaks (2,700 cm^{-1}), respectively. The disorder-induced D peak is not apparent in pristine graphene because of crystal symmetry, while the G peak, which is the primary

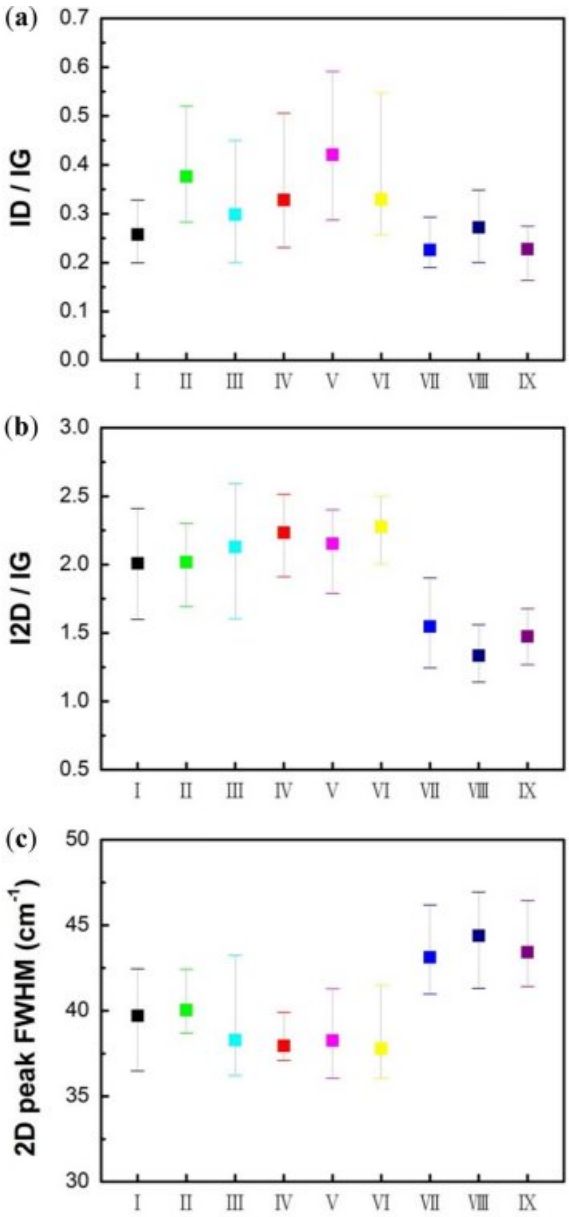

Fig. 4. Raman spectral data of graphene synthesized in nine different gas conditions. (a) I_D/I_G ratio, (b) I_{2D}/I_G ratio, and (c) 2D peak FWHM.

in-plane vibrational mode according to the bond stretching in both rings and chains, was derived from all pairs of sp^2-hybridized carbon atoms. One way to characterize the disorder and defect levels of graphene is to use Raman spectra for the intensity ratio (I_D/I_G) of the D peak to G peak. Furthermore, the 2D peak is owing to double resonance, which links the phonon wave vectors to the electronic band structure. In addition, near the K point containing the phonon, the 2D peak occurs as a result of the 2-phonon resonance process. The 2D peak is very prominent in graphene than in bulk graphite.

Graphene can be deduced from the number of layers of graphene using the intensity ratio of 2D peak to G peak (I_{2D}/I_G). The I_{2D}/I_G ratio of pristine single-layer

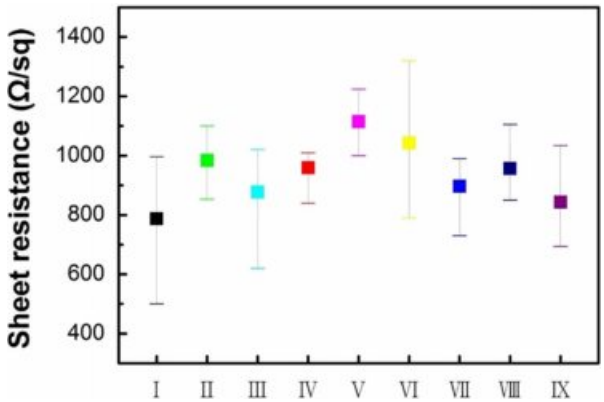

Fig. 5. Sheet resistance of graphene synthesized in nine different gas conditions.

graphene was 3.4 [25-31]. In this study, Raman ratio was directly obtained from the statistical analysis with 20 points. The I_D/I_G ratios of samples I (0.258), VII (0.226), VIII (0.272), and IX (0.228) were lower than that of the other samples. Formation of multi-layer graphene domains with hydrogen pretreatment, and low I_D/I_G ratios were calculated for samples VII, VIII, and IX. Among the samples synthesized under the same gas conditions in Step2, the strongest D peak appeared for the sample for which argon was introduced in Step4.

The absence of a reducing gas such as hydrogen and methane to protect from oxidizing impurities promote defects [31].

The average value of I_{2D}/I_G ratio of graphene and the full width at half maximum (FWHM) of the 2D peak distinguished the graphene layer [27]. Samples VII, VIII, and IX exhibited lower I_{2D}/I_G ratios and higher FWHM values than those of the samples prepared in other conditions.

Fig. 5 shows the graphene sheet resistance to nine graphene synthesis gas conditions. The lowest average sheet resistance of 787.49 Ω/sq was measured for sample 1. Among the samples synthesized under the same gas conditions in Step2, the highest sheet resistance was recorded for the sample for which argon was introduced in Step4. The trend of sheet resistance (Fig. 5) is similar to that of I_D/I_G ratio (Fig. 4 (a)). Further, the relatively poor electrical conductivity of graphene is due to structural defects formed during the synthesis process [10].

Conclusion

Graphene synthesis using RT-CVD under various gas conditions and hydrogen pre-treatment in Step2 led to the growth of multi-layer graphene domains. On the other hand, the absence of a reducing gas promoted defects, which led to the degradation of electrical characteristics. The flow of methane in Step2 and Step4 during graphene synthesis by RT-CVD caused less degradation of electrical properties and provided optical properties similar to that of pristine graphene.

Acknowledgment

This work was supported by the "World Class 300 Project (R&D) (S2561932)" of the MOTIE, MSS (Korea). This work was supported by the Ministry of Trade, Industry and Energy through Technology Innovation Program (Grant No. 10067449). This work was partly supported by the GRRC program of Gyeonggi province [GRRC Sungkyunkwan 2017-B03, Development of chemical sensor based on metal oxide materials]. This work was supported by the Korea Basic Science Institute (KBSI) National Research Facilities & Equipment Center (NFEC) grant funded by the Korea government (Ministry of Education) (No. 2019R1A6C1010031).

Acknowledgment

†Y.S. Lee, †D.I. Jeong, and †Y. Yoon contributed equally to this work. †Y.S. Lee, †D.I. Jeong, and †Y. Yoon designed and wrote this study.

References

1. K.S. Novoselov, V. Fal, L. Colombo, P. Gellert, M. Schwab, and K. Kim, Nature 490[7419] (2012) 192-200.
2. O.C. Compton and S.T. Nguyen, Small 6[6] (2010) 711-723.
3. C. Lee, X. Wei, J.W. Kysar, and J. Hone, Science 321[5887] (2008) 385-388.
4. M. Pumera, Energy Environ. Sci. 4[3] (2011) 668-674.
5. X. Wang, L. Zhi, and K. Müllen, Nano Lett. 8[1] (2008) 323-327.
6. X. Yang, J. Zhu, L. Qiu, and D. Li, Adv. Mater. 23[25] (2011) 2833-2838.
7. V. Goyal and A.A. Balandin, Appl. Phys. Lett. 100[7] (2012) 073113.
8. M.I. Katsnelson, Mater. Today 10[1-2] (2007) 20-27.
9. A.C. Neto, F. Guinea, N.M. Peres, K.S. Novoselov, and A.K. Geim, Rev. Mod. Phys. 81[1] (2009) 109-162.
10. K.S. Kim, Y. Zhao, H. Jang, S.Y. Lee, J.M. Kim, K.S. Kim, J.-H. Ahn, P. Kim, J.-Y. Choi, and B.H. Hong, Nature 457[7230] (2009) 706-710.
11. A. Reina, X. Jia, J. Ho, D. Nezich, H. Son, V. Bulovic, M.S. Dresselhaus, and J. Kong, Nano Lett. 9[1] (2008) 30-35.
12. M. Losurdo, M.M. Giangregorio, P. Capezzuto, and G. Bruno, Phys. Chem. Chem. Phys., 13[46] (2011) 20836-20843.
13. C. Mattevi, H. Kim, and M. Chhowalla, J. Mater. Chem. 21[10] (2011) 3324-3334.
14. X. Li, Y. Zhu, W. Cai, M. Borysiak, B. Han, D. Chen, R.D. Piner, L. Colombo, and R.S. Ruoff, Nano Lett. 9[12] (2009) 4359-4363.
15. J. Ryu, Y. Kim, D. Won, N. Kim, J.S. Park, E.-K. Lee, D. Cho, S.-P. Cho, S.J. Kim, and G.H. Ryu, ACS Nano 8[1] (2014) 950-956.
16. F. Banhart, J. Kotakoski, and A.V. Krasheninnikov, ACS Nano 5[1] (2010) 26-41.

17. A. Hashimoto, K. Suenaga, A. Gloter, K. Urita, and S. Iijima, Nature 430[7002] (2004) 870-873.
18. S. Bhaviripudi, X. Jia, M.S. Dresselhaus, and J. Kong, Nano Lett. 10[10] (2010) 4128-4133.
19. Y. Hao, M. Bharathi, L. Wang, Y. Liu, H. Chen, S. Nie, X. Wang, H. Chou, C. Tan, B. Fallahazad, H. Ramanarayan, C. W. Magnuson, E. Tutuc, B. I. Yakobson, K. F. McCarty, Y.-W. Zhang, P. Kim, J. Hone, L. Colombo, and R. S. Ruoff, Science 342[6159] (2013) 720-723.
20. X. Li, W. Cai, J. An, S. Kim, J. Nah, D. Yang, R. Piner, A. Velamakanni, I. Jung, E. Tutuc, E. Tutuc, S. K. Banerjee, L. Colombo, and R. S. Ruoff, Science 324[5932] (2009) 1312-1314.
21. I. Vlassiouk, M. Regmi, P. Fulvio, S. Dai, P. Datskos, G. Eres, and S. Smirnov, ACS Nano 5[7] (2011) 6069-6076.
22. X. Li, C.W. Magnuson, A. Venugopal, R.M. Tromp, J.B. Hannon, E.M. Vogel, L. Colombo, and R.S. Ruoff, J. Am. Chem. Soc. 133[9] (2011) 2816-2819.
23. L. Tao, J. Lee, H. Chou, M. Holt, R.S. Ruoff, and D. Akinwande, ACS Nano 6[3] (2012) 2319-2325.
24. R.R. Nair, P. Blake, A.N. Grigorenko, K.S. Novoselov, T.J. Booth, T. Stauber, N.M. Peres, and A.K. Geim, Science 320[5881] (2008) 1308-1308.
25. D. Yoon, Y.-W. Son, and H. Cheong, Phys. Rev. Lett. 106[15] (2011) 155502.
26. Z. Ni, Y. Wang, T. Yu, and Z. Shen, Nano Res. 1[4] (2008) 273-291.
27. Y. Hao, Y. Wang, L. Wang, Z. Ni, Z. Wang, R. Wang, C.K. Koo, Z. Shen, and J.T. Thong, Small 6[2] (2010) 195-200.
28. D.R. Cooper, B. D'Anjou, N. Ghattamaneni, B. Harack, M. Hilke, A. Horth, N. Majlis, M. Massicotte, L. Vandsburger, and E. Whiteway, ISRN Condens. Matter Phys. 2012 (2012) 1-56.
29. I. Childres, L.A. Jauregui, J. Tian, W. Park, H. Cao, and Y.P. Chen, New Developments in Photon and Materials Research 1. 13[2] (2013) 025008.
30. C. Casiraghi, S. Pisana, K. Novoselov, A. Geim, and A. Ferrari, Appl. Phys. Lett. 91[23] (2007) 233108.
31. S. Choubak, P.L. Levesque, E. Gaufres, M. Biron, P. Desjardins, and R. Martel, J. Phys. Chem. C 118[37] (2014) 21532-21540.